Inorg. Chem. **2007**, *46*, 6170–6177

$Rb_3Ti_3(P_4S_{13})(PS_4)_3$ and $Cs_2Ti_2(P_2S_8)(PS_4)_2$: Two Polar Titanium Thiophosphates with Complex One-Dimensional Tunnels

Yuandong Wu and Wolfgang Bensch*

Institut für Anorganische Chemie, Universität Kiel, Olshausenstrasse 40, D24098 Kiel, Germany

Received March 12, 2007

The reactions of Ti with in situ formed polythiophosphate fluxes of A_2S_3 (A = Rb, Cs), P_2S_5, and S at 500 °C result in the formation of two new quaternary titanium thiophosphates with compositions $Rb_3Ti_3(P_4S_{13})(PS_4)_3$ (**1**) and $Cs_2Ti_2(P_2S_8)(PS_4)_2$ (**2**). $Rb_3Ti_3(P_4S_{13})(PS_4)_3$ (**1**) crystallizes in the chiral hexagonal space group $P6_3$ (No. 173) with lattice parameters $a = 18.2475(9)$ Å, $c = 6.8687(3)$ Å, $V = 1980.7(2)$ Å^3, $Z = 2$. $Cs_2Ti_2(P_2S_8)(PS_4)_2$ (**2**) crystallizes in the noncentrosymmetric monoclinic space group *Cc* (No. 9) with $a = 21.9709(14)$ Å, $b = 6.9093(3)$ Å, $c = 17.1489(10)$ Å, $\beta = 98.79(1)°$, $V = 2572.7(2)$ Å^3, $Z = 4$. In the structure of **1** TiS_6 octahedra, three $[PS_4]$ tetrahedra, and the hitherto unknown $[P_4S_{13}]^{6-}$ anion are joined to form two different types of helical chains. These chains are connected yielding two different helical tunnels being directed along [001]. The tunnels are occupied by the Rb^+ ions. The $[P_4S_{13}]^{6-}$ anion is generated by three $[PS_4]$ tetrahedra sharing corners with one $[PS_4]$ group in the center of the starlike anion. The P atoms of the three $[PS_4]$ tetrahedra attached to the central $[PS_4]$ group define an equilateral triangle. The $[P_4S_{13}]^{6-}$ anion may be regarded as a new member of the $[P_nS_{3n+1}]^{(n+2)-}$ series. The structure of $Cs_2Ti_2(P_2S_8)(PS_4)_2$ (**2**) consists of the one-dimensional polar tunnels containing the Cs^+ cations. The rare $[P_2S_8]^{4-}$ anion which is composed of two $[PS_4]$ tetrahedra joined by a S_2^{2-} anion is a fundamental building unit in the structure of **2**. One-dimensional undulated chains being directed along [100] are joined by $[PS_4]$ tetrahedra to form the three-dimensional network with polar tunnels running along [010]. The compounds are characterized with IR, Raman spectroscopy, and UV/vis diffuse reflectance spectroscopy.

1. Introduction

A large number of new and complex compounds were prepared applying chalcophosphate fluxes. These compounds often show elaborate structure types arising from the large variety of new binding modes displayed by the $[P_xQ_y]_m^{n-}$ (Q = S, Se) building blocks.[1] The polychalcophosphate fluxes are formed by the in situ fusion of A_2Q_x, P_2Q_5, and Q (A = alkali metal; Q = S, Se) and contain various highly reactive $[P_xQ_y]^{n-}$ species available for the reaction with metal ions. Until now only a few quaternary alkali metal group 4 chalcophosphates like $NaTi_2(PS_4)_3$,[2] $ATiPQ_5$ (A = K, Rb; Q = S, Se),[3] $K_4Ti_2P_6S_{25}$ and $K_3Ti_2P_5S_{18}$,[4] $Rb_4Ti_2P_6Se_{25}$,[3b] $A_3Zr_2P_5S_{18}$ (A = Rb, Cs),[5] $Cs_3Hf_2P_5S_{18}$,[6] and the three silver compounds $AgTi_2(PS_4)_3$, $Ag_2NbTi_3P_6S_{25}$,[7] and $Ag_2Ti_2P_2S_{11}$[8] have been reported. The dimensionality of the structures varies from one-dimensional chains to three-dimensional networks. In these thiophosphates the TiS_6 octahedra or MS_7 (M = Zr, Hf) pentagonal bipyramids share common corners, edges, or faces with other MS_6 octahedra and/or different $[P_xS_y]$ anions generated from the $[PS_4]$. The $[P_2Q_7]^{4-}$ and $[P_2Q_9]^{4-}$ anions are found in $A_4Ti_2P_6Q_{25}$ (A = K, Rb; Q = S, Se,[3b,4] whereas $K_3Ti_2P_5S_{18}$[4] contains $[PS_4]^{3-}$ and $[P_2S_7]^{4-}$ anions. A combination of $[P_2S_6]^{2-}$ and $[PS_4]^{3-}$ ions is observed in $Ag_2NbTi_3P_6S_{25}$.[7] Finally, in the compounds A_3-

* To whom correspondence should be addressed. E-mail: wbensch@ac.uni-kiel.de. Fax: +49-431-8801520.

(1) (a) Kanatzidis, M. G. *Curr. Opin. Solid State Mater. Sci.* **1997**, *2*, 139−149. (b) Sutorik, A. C.; Kanatzidis, M. G. *Prog. Inorg. Chem.* **1995**, *43*, 151−265.
(2) Cieren, X.; Angenault, J.; Couturier, J.-C.; Jaulmes, S.; Quarton, M.; Robert, F. *J. Solid State Chem.* **1996**, *121*, 230−235.
(3) (a) Do, J.; Lee, K.; Yun, H. *J. Solid State Chem.* **1996**, *125*, 30−36. (b) Chondroudis, K.; Kanatzidis, M. G. *Inorg. Chem.* **1995**, *34*, 5401−5402.
(4) Derstroff, V.; Tremel, W.; Regeldky, G.; Schmedt auf der Günne, J.; Eckert, H. *Solid State Sci.* **2002**, *4*, 731−745.
(5) Gutzmann, A.; Näther, C.; Bensch, W. *Solid State Sci.* **2004**, *6*, 205−211.
(6) Gutzmann, A.; Näther, C.; Bensch, W. *Acta Crystallogr.* **2004**, *E60*, i42−i44.
(7) Angenault, J.; Cieren, X.; Wallez, G.; Quarton, M. *J. Solid State Chem.* **2000**, *153*, 55−65.
(8) Gaudin, E.; Fischer, L.; Boucher, F.; Evain, M.; Petricek, M. *Acta Cryst.* **1997**, *B53*, 67−75.

10.1021/ic700478r CCC: $37.00
Published on Web 06/21/2007

$Zr_2P_5S_{18}$ (A = Rb, Cs)[5] and $Cs_3Hf_2P_5S_{18}$[6] $[PS_4]^{3-}$ and $[P_2S_7]^{4-}$ anions coexist. The incorporation of alkali metals generally induces a decrease of the dimensionality of the anionic networks.

In our ongoing explorative work in the quaternary alkali metal group 4 chalcophosphate system the two new compounds $Rb_3Ti_3(P_4S_{13})(PS_4)_3$ and $Cs_2Ti_2(P_2S_8)(PS_4)_2$ are obtained in high yields. In the contribution the syntheses, crystal structures, and optical properties are presented.

2. Experimental Section

2.1. Reagents. The following reagents were used as purchased: Cs (99.5%, Strem), Ti (99.97%, Fluka), P_2S_5 (99.99%, Alfa), and S (99.99%, Heraeus).

2.2. Syntheses. A_2S_3 (A = Rb, Cs) were prepared from a stoichiometric mixture of the elements in liquid ammonia under an argon atmosphere.

After the reactions the excess $A_x[P_yS_z]$ (A = Rb, Cs) fluxes were removed by washing with DMF and acetone. Both compounds are stable in air for several months but decompose in the presence of water.

Preparation of $Rb_3Ti_3(P_4S_{13})(PS_4)_3$ (1). Rb_2S_3 (0.087 g, 0.33 mmol), Ti (0.016 g, 0.33 mmol), P_2S_5 (0.145 g, 0.65 mmol), and S (0.052 g, 1.63 mmol) were thoroughly mixed in a N_2-filled glovebox and loaded into glass (Duran) tubes which were evacuated (1×10^{-3} mbar) and flame-sealed. The ampoules were placed in a computer controlled furnace and heated to 500 °C within 24 h. After 6 days the samples were cooled down to 100 °C at a rate of 2 °C/h followed by cooling to room temperature in 4 h. The product consists of black crystals (95% yield based on Ti).

Preparation of $Cs_2Ti_2(P_2S_8)(PS_4)_2$ (2). A mixture of Cs_2S_3 (0.107 g, 0.30 mmol), Ti (0.014 g, 0.30 mmol), P_2S_5 (0.131 g, 0.60 mmol), and S (0.047 g, 1.50 mmol) was sealed under vacuum in a Duran glass tube. The mixture was heated to 500 °C for 5 days, followed by cooling to 100 °C at a rate of 2 °C/h. The product contained black crystals (90% yield based on Ti).

2.3. Physical Measurements. Infrared Spectroscopy. Infrared spectra in the MIR region (4000−400 cm^{-1}, 2 cm^{-1} resolution) were recorded on a Genesis FT-spectrometer (ATI Mattson). The samples were ground with dry KBr into fine powders and pressed into transparent pellets. Infrared spectra in the far-IR region (550−80 cm^{-1}) were collected on an ISF-66 device (Bruker) with the samples pressed in polyethylene pellets.

Raman Spectroscopy. Raman spectra were recorded on an ISF-66 spectrometer (Bruker) equipped with an additional FRA 106 Raman module. A Nd/YAG laser was used as source (λ = 1064 nm). The samples were ground and prepared on Al sample holders. The measuring range was −1000 to 3500 cm^{-1} (resolution: 2 cm^{-1}).

Solid-State Ultraviolet (UV)−Visible (Vis)−Near-IR Spectroscopy. Optical diffuse reflectance measurements were performed at room temperature using a UV−vis-NIR two-channel spectrometer Cary 5 from Varian Techtron Pty., Darmstadt. The spectrometer is equipped with an Ulbricht sphere (Diffuse reflectance accessory; Varian Techtron Pty.). The inner wall of the Ulbricht sphere (diameter 110 mm) is covered with a PTFE layer of 4 mm thickness. A PbS detector (NIR) and a photomultiplier (UV/vis) are attached to the Ulbricht sphere. The samples were ground with $BaSO_4$ (standard for 100% reflectance) and prepared as a flat specimen. The resolution was 1 nm for the UV/vis range and 2 nm for the near-IR range. The measuring range was 250−2000 nm. Absorption (α/S) data were calculated from the reflectance spectra using the Kubelka−Munk function,[9] $\alpha/S = (1-R)^2/2R$, where R is the reflectance at a given wavenumber, α is the absorption coefficient, and S is the scatting coefficient. The band gap was determined as the intersection point between the energy axis at the absorption offset and the line extrapolated from the linear part of the absorption edge in a $(\alpha/S)^2$ versus E (eV) plot.

Microprobe Analyses. Microprobe analyses were performed with a Philips ESEM XL 30 scanning electron microscope equipped with an EDAX analyzer. The compositions reported here are the result of averaging a large number of independent measurements from a given samples. The EDX data yield an atomic ratio of 1.2:1:2.5:8.5 (Rb:Ti:P:S) for compound **1** and 1.1:1:2:7.5 (Cs:Ti:P:S) for compound **2**.

Single-Crystal X-ray Crystallography. Data sets of both compounds were collected on a STOE Imaging Plate Diffraction System (IPDS-1) with graphite monochromatized Mo Kα radiation (λ = 0.7107 Å). Size of crystal **1**: $0.13 \times 0.09 \times 0.08$ mm^3; crystal **2**: $0.12 \times 0.09 \times 0.05$ mm^3. The raw intensities were corrected for Lorentz, polarization, and absorption. The structure was solved with direct methods and refined with full matrix least-squares techniques using the SHELXTL software package.[10]

$Rb_3Ti_3(P_4S_{13})(PS_4)_3$. The Rb(2) atom showed an abnormally high displacement parameter (ADP), implying a partial occupancy of this site. The refined occupancy for Rb(2) was 0.101(2) yielding the nominal composition $Rb_{3.30}Ti_3P_7S_{25}$, which does not satisfy charge neutrality. To achieve charge neutrality the sum of occupancies of Rb(1) and Rb(2) was constrained. The introduction of this constraint yields significantly lower displacement parameters and final occupancies for Rb(1) and Rb(2) of 0.906(1) and 0.281(4), respectively.

An attempt to solve the structure in the centrosymmetric space group $P6_3/m$ failed. A symmetry check was performed with the ADDSYM option[11] in PLATON[12] giving no hint for the presence of a mirror plane. The absolute structure was determined and is in agreement with the selected setting (Flack x parameter: −0.015(9)).

$Cs_2Ti_2(P_2S_8)(PS_4)_2$. The structure was solved and refined successfully in the space group Cc. A check with PLATON[12] gives no hints for a higher symmetry. The selected setting is in agreement with the Flack x parameter of −0.018(14).

Technical details of the data acquisition as well as selected refinement results for $Rb_3Ti_3P_7S_{25}$ (**1**) and $CsTiP_2S_8$ (**2**) are summarized in Table 1. Selected bond distances are listed in Tables 2 (**1**) and 3 (**2**).

3. Results and Discussion

3.1. Crystal Structures. The three-dimensional network of $Rb_3Ti_3(P_4S_{13})(PS_4)_3$ is constructed by the interconnection of $[TiS_6]$ octahedra and two types of thiophosphate ligands, $[PS_4]^{3-}$, and the previously unknown $[P_4S_{13}]^{6-}$ anion. This anion is composed of four corner-sharing $[PS_4]$ tetrahedra with a starlike shape, i.e., the central $[P(1)S_4]$ tetrahedron is joined to three symmetry related $[P(3)S_4]$ tetrahedral (Figure 1, top). Two different types of one-dimensional tunnels are formed hosting the Rb^+ cations (Figure 1, bottom). Tunnel **I** with a round shape is formed by $[TiS_6]$ octahedra and $[PS_4]$

(9) Kulbelka, P.; Munk, F. *Z. Tech. Phys.* **1931**, *12*, 593−601.
(10) Sheldrick, G. M. *SHELXTL Version 5.1*; Bruker AXS Inc.: Madison, WI, U.S.A., 1998.
(11) Le Page, Y. *J. Appl. Crystallogr.* **1988**, *21*, 983−984.
(12) (a) Spek, A. L. *Platon, A Multipurpose Crystallographic Tool*; Utrecht University: The Netherlands, 2007. (b) Spek, A. L. *J. Appl. Crystallogr.* **2003**, *36*, 7−13.

Table 1. Crystal Data and Selected Refinement Results for $Rb_3Ti_3(P_4S_{13})(PS_4)_3$ (**1**) and $Cs_2Ti_2(P_2S_8)(PS_4)_2$ (**2**)

	$Rb_3Ti_3(P_4S_{13})(PS_4)_3$	$Cs_2Ti_2(P_2S_8)(PS_4)_2$
Fw	1418.40	998.46
space group	$P6_3$	Cc
a (Å)	18.2475(9)	21.9709(14)
b (Å)	18.2475(9)	6.9093(3)
c (Å)	6.8687(3)	17.1489(10)
β (deg)		98.785(7)
V (Å^3)	1980.67(16)	2572.7(2)
Z	2	4
T (K)	180	220
D_{calc} (g/cm^3)	2.378	2.578
μ (mm^{-1})	5.862	4.949
index range	$-21 \le h \le 24$	$-28 \le h \le 28$
	$-24 \le k \le 24$	$-9 \le k \le 9$
	$-8 \le l \le 8$	$-22 \le l \le 22$
$2\theta_{max}$ (deg)	56	56
R_{int}	0.0522	0.0486
R1 ($F_o > 4\sigma(F_o)$)	0.0318	0.0337
wR2 (all data)	0.0754	0.0801
GOOF	1.022	0.973
$\Delta\rho$ [e Å^{-3}]	0.571/−0.533	0.994/−0.818

Table 2. Selected Distances (Å) and Angles (deg) for $Rb_3Ti_3(P_4S_{13})(PS_4)_3$ (**1**)

Distances (Å)

Ti(1)−S(5)	2.3938(15)	Ti(1)−S(7)	2.4108(13)
Ti(1)−S(3)	2.4121(14)	Ti(1)−S(1)	2.4189(13)
Ti(1)−S(2)	2.4547(13)	Ti(1)−S(4)	2.4659(14)
P(1)−S(9)	1.935(3)	P(1)−S(6)	2.1009(15)×3
P(2)−S(7)	2.0243(17)	P(2)−S(5)	2.0272(15)
P(2)−S(3)	2.0398(15)	P(2)−S(1)	2.0409(16)
P(3)−S(8)	1.9533(15)	P(3)−S(2)	2.0347(18)
P(3)−S(4)	2.0380(16)	P(3)−S(6)	2.1726(15)

Angles (deg)

S(5)−Ti(1)−S(7)	90.47(5)	S(5)−Ti(1)−S(3)	100.03(5)
S(7)−Ti(1)−S(3)	82.52(4)	S(5)−Ti(1)−S(1)	82.65(4)
S(7)−Ti(1)−S(1)	168.99(5)	S(3)−Ti(1)−S(1)	90.20(4)
S(5)−Ti(1)−S(2)	90.34(5)	S(7)−Ti(1)−S(2)	83.82(5)
S(3)−Ti(1)−S(2)	162.88(5)	S(1)−Ti(1)−S(2)	104.72(5)
S(5)−Ti(1)−S(4)	163.89(5)	S(7)−Ti(1)−S(4)	102.53(5)
S(3)−Ti(1)−S(4)	91.16(5)	S(1)−Ti(1)−S(4)	85.78(4)
S(2)−Ti(1)−S(4)	81.79(4)	S(9)−P(1)−S(6)	117.71(6)
S(9)−P(1)−S(6)	117.71(6)	S(6)−P(1)−S(6)	100.12(8)
S(9)−P(1)−S(6)	117.71(6)	S(6)−P(1)−S(6)	100.12(8)
S(6)−P(1)−S(6)	100.12(8)	S(7)−P(2)−S(5)	114.68(8)
S(7)−P(2)−S(3)	102.99(6)	S(5)−P(2)−S(3)	112.49(7)
S(7)−P(2)−S(1)	110.39(7)	S(5)−P(2)−S(1)	102.75(7)
S(3)−P(2)−S(1)	113.93(7)	S(8)−P(3)−S(2)	115.67(8)
S(8)−P(3)−S(4)	117.55(8)	S(2)−P(3)−S(4)	104.55(6)
S(8)−P(3)−S(6)	111.71(7)	S(2)−P(3)−S(6)	109.51(7)
S(4)−P(3)−S(6)	95.89(7)		

Table 3. Selected Distances (Å) and Angles (deg) for $Cs_2Ti_2(P_2S_8)(PS_4)_2$ (**2**)

Distances (Å)

Ti(1)−S(7)	2.4103(18)	Ti(1)−S(13)	2.4106(18)
Ti(1)−S(14)	2.4257(19)	Ti(1)−S(9)	2.4433(18)
Ti(1)−S(10)	2.4560(18)	Ti(1)−S(8)	2.4659(18)
Ti(2)−S(16)	2.4159(18)	Ti(2)−S(15)	2.4204(19)
Ti(2)−S(11)	2.4302(18)	Ti(2)−S(2)	2.4372(19)
Ti(2)−S(12)	2.4380(19)	Ti(2)−S(1)	2.4474(18)
P(1)−S(3)	1.954(2)	P(1)−S(1)	2.038(2)
P(1)−S(2)	2.047(2)	P(1)−S(4)	2.132(2)
P(2)−S(6)	1.957(2)	P(2)−S(7)	2.049(2)
P(2)−S(8)	2.050(2)	P(2)−S(5)	2.140(2)
P(3)−S(11)	2.035(2)	P(3)−S(9)	2.037(2)
P(3)−S(12)	2.040(2)	P(3)−S(10)	2.042(2)
P(4)−S(14)	2.029(2)	P(4)−S(16)	2.032(2)
P(4)−S(13)	2.038(2)	P(4)−S(15)	2.043(2)
S(4)−S(5)	2.033(2)		

Angles (deg)

S(7)−Ti(1)−S(13)	100.18(7)	S(7)−Ti(1)−S(14)	97.33(6)
S(13)−Ti(1)−S(14)	80.51(6)	S(7)−Ti(1)−S(9)	158.53(7)
S(13)−Ti(1)−S(9)	96.87(6)	S(14)−Ti(1)−S(9)	98.28(6)
S(7)−Ti(1)−S(10)	86.78(6)	S(13)−Ti(1)−S(10)	159.18(7)
S(14)−Ti(1)−S(10)	79.15(6)	S(9)−Ti(1)−S(10)	81.78(6)
S(7)−Ti(1)−S(8)	80.97(6)	S(13)−Ti(1)−S(8)	90.85(6)
S(14)−Ti(1)−S(8)	170.79(7)	S(9)−Ti(1)−S(8)	85.85(6)
S(10)−Ti(1)−S(8)	109.69(7)	S(16)−Ti(2)−S(15)	82.41(6)
S(16)−Ti(2)−S(11)	98.01(7)	S(15)−Ti(2)−S(11)	85.77(6)
S(16)−Ti(2)−S(2)	88.53(6)	S(15)−Ti(2)−S(2)	107.60(7)
S(11)−Ti(2)−S(2)	165.86(8)	S(16)−Ti(2)−S(12)	93.66(7)
S(15)−Ti(2)−S(12)	165.74(7)	S(11)−Ti(2)−S(12)	81.19(6)
S(2)−Ti(2)−S(12)	85.91(7)	S(16)−Ti(2)−S(1)	162.37(7)
S(15)−Ti(2)−S(1)	85.74(6)	S(11)−Ti(2)−S(1)	94.07(6)
S(2)−Ti(2)−S(1)	82.65(6)	S(12)−Ti(2)−S(1)	100.87(7)
S(3)−P(1)−S(1)	117.40(11)	S(3)−P(1)−S(2)	115.75(10)
S(1)−P(1)−S(2)	104.29(9)	S(3)−P(1)−S(4)	111.97(10)
S(1)−P(1)−S(4)	96.59(9)	S(2)−P(1)−S(4)	108.91(10)
S(6)−P(2)−S(7)	119.97(11)	S(6)−P(2)−S(8)	116.63(10)
S(7)−P(2)−S(8)	101.12(9)	S(6)−P(2)−S(5)	112.25(10)
S(7)−P(2)−S(5)	95.57(9)	S(8)−P(2)−S(5)	108.82(10)
S(11)−P(3)−S(9)	113.34(10)	S(11)−P(3)−S(12)	102.04(9)
S(9)−P(3)−S(12)	110.1(1)	S(11)−P(3)−S(10)	111.67(10)
S(9)−P(3)−S(10)	103.70(9)	S(12)−P(3)−S(10)	116.42(10)
S(14)−P(4)−S(16)	116.2(1)	S(14)−P(4)−S(13)	100.41(9)
S(16)−P(4)−S(13)	114.07(9)	S(14)−P(4)−S(15)	111.05(9)
S(16)−P(4)−S(15)	102.83(9)	S(13)−P(4)−S(15)	112.73(10)
S(5)−S(4)−P(1)	104.14(10)	S(4)−S(5)−P(2)	106.51(9)

units in the following way. The [TiS_6] octahedra share two edges with the [$P(2)S_4$]$^{3-}$ tetrahedra (see Figure 2, top) in the sequence −P(2)-Ti−P(2)−Ti−P(2)− yielding an infinite helical chain which is directed along the *c*-axis. An inspection of the structure shows that three such helical chains propagate along [001] and coil around each other to form the type **I** tunnel (Figure 2, bottom). The shortest S−S distance between these chains is 3.261(2) Å which is too long for bonding interactions. Four such tunnels are located around the 6_3 axes of the hexagonal unit cell. Adjacent tunnels share edges with the three $P(3)S_4$ tetrahedra of the [P_4S_{13}]$^{6-}$ anion thus forming another kind of helical chain being also directed along [001], i.e., each [P_4S_{13}]$^{6-}$ anion joins three tunnels of type **I** (compare Figure 1). The sequence within this helical chain is −Ti−P(2)−Ti−P(3)−P(1)−P(3)−Ti−P(2)−Ti− (Figure 3, top). The helical chains create the helical tunnel **II** with an elliptical shape (Figure 3, bottom). Tunnel **I** is surrounded by six tunnels of type **II**. Because there is no S−S bonding in the structure, the electronic situation of the compound may be described as [Rb^+]$_3$[Ti^{4+}]$_3$[PS_4^{3-}]$_3$[$P_4S_{13}^{6-}$].

The Ti−S bond lengths range from 2.3938(15) to 2.4659(14) Å with an average of 2.4260(14) Å comparing well with the value of 2.427 Å for TiS_2.[13] The S−Ti−S angles clearly indicate a strong distortion of the octahedron which may be caused by the bonding requirements of the thiophosphate groups. In the basal plane the S−Ti−S angles scatter between 81.79(4) and 163.89(5)° (Table 2). The new [P_4S_{13}]$^{6-}$ unit is the fundamental building block of the structure and is formed by four [PS_4] tetrahedra sharing corners with the [$P(1)S_4$] tetrahedron being the center of a star. The three P(3) atoms of the [P_4S_{13}]$^{6-}$ unit define an equilateral triangle (P−P distance: 5.944(2) Å) with the P(1) atom being located in the center of the triangle. The P−S bond lengths in the

(13) Kusawake, T.; Takahashi, Y.; Wey, M.-Y.; Ohshima, K.-I. *J. Phys.: Condens. Matter.* **2001**, *13*, 9913−9922.

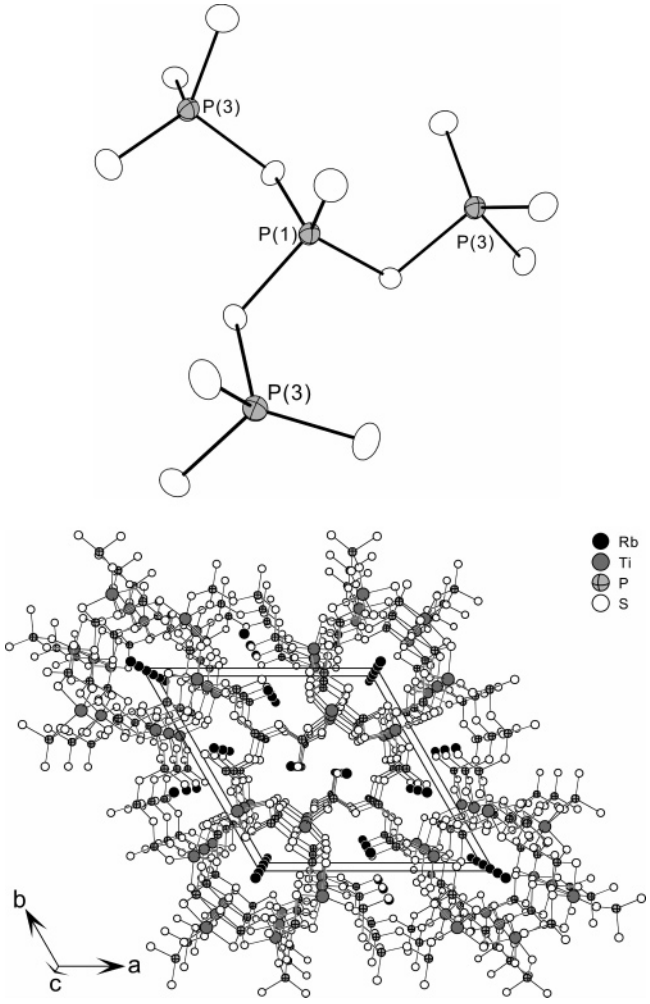

Figure 1. The $[P_4S_{13}]^{6-}$ anion in $Rb_3Ti_3(P_4S_{13})(PS_4)_3$ (top; probability ellipsoids are presented on the 70% level) and the crystal structure viewed along [001].

$[P_4S_{13}]^{6-}$ anion range from 1.935(3) to 2.173(2) Å (average bond lengths: 2.060(3) for P(1), 2.050(3) Å for P(3)). The mean values are in good agreement with the sum of the ionic radii (rP^{5+} = 0.17 Å, rS^{2-} = 1.84 Å).[14] There are three groups of P−S bond lengths in the $[P_4S_{13}]^{6-}$ anion: (i) P−S(8, 9) bonds to terminal S atoms at 1.953(2) and 1.936(3) Å; (ii) P(3)−S(2, 4) bonds with 2.035(2) and 2.038(2) Å which are to S atoms having also a bond to the Ti atom; and (iii) the P−S(6) bonds of 2.101(2) and 2.173(2) Å to S atoms bridging different PS_4 tetrahedra. A similar trend of the P−S bond lengths was observed in the structures of $K_4Ti_2P_6S_{25}$ and $K_3Ti_2P_5S_{18}$[4]. The S−P−S angles reveal an obvious deviation from the tetrahedral geometry (range: 95.9(1)−117.7(1)°).

The $[P_4S_{13}]^{6-}$ unit represents a new member of the $[P_nS_{3n+1}]^{(n+2)-}$ series including the pyrothiophosphates $[P_2S_7]^{4-}$[15] and $[P_3S_{10}]^{5-}$.[16] We note that the ternary sulfide $V_2P_4S_{13}$[17] contains an anion with the same formula as in **1** but the $[P_4S_{13}]$ group is a straight chain composed of four $[PS_4]$ tetrahedra, whereas the $[P_4S_{13}]^{6-}$ anion in $Rb_3Ti_3(P_4S_{13})(PS_4)_3$ is formed by a central $[PS_4]$ tetrahedron joined

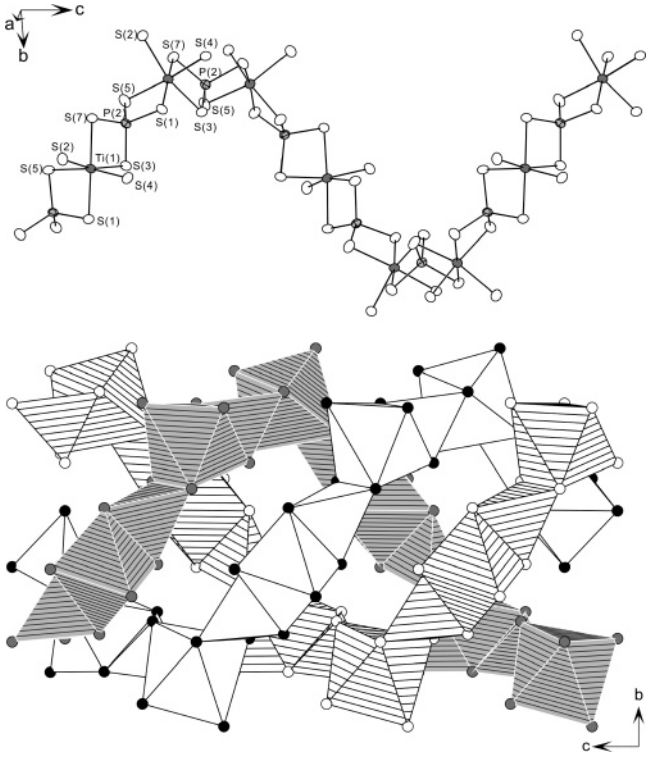

Figure 2. The anionic chain in $Rb_3Ti_3(P_4S_{13})(PS_4)_3$ with atomic labeling (top). Polyhedral representation of the three independent helical chains running along [001] coiling around each other to form tunnel **I** (bottom). The polyhedra in the three chains are drawn with different shadings, and Rb^+ ions are omitted for clarity. The ellipsoids are drawn at the 70% probability level.

to three other $[PS_4]$ groups via common corners. Considering the structure of the anion one can start with the adamantine-like cage of P_4S_{10}.[18] The structure of the $[P_4S_{13}]^{6-}$ anion is then derived by opening of the P_4S_{10} unit through the insertion of three S^{2-} ions (see Scheme 1). Formally, this process leads one unchanged $[PS_4]$ tetrahedron, and the remaining P_3S_3 ring is then opened to form three other $[PS_4]$ groups.

The tunnels in **1** contain the Rb^+ cations that are located on two different sites. Rb(1) resides in tunnel **II** and is in a 9-fold coordination of S atoms (range of Rb(1)−S distances: 3.405(1) to 3.919(1) Å; average 3.634(1) Å), and the Rb(2) atom in tunnel **I** is octahedrally surrounded by 6 S atoms (range: 3.617(3) to 3.621(3) Å; average 3.619(3) Å). The $Rb(2)S_6$ octahedra share common triangular faces along [001].

(14) Shannon, R. D. *Acta Crystallogr., Sect. A: Found. Crystallogr.* **1976**, *A32*, 751−767.

(15) (a) Menzel, F.; Ohse, L.; Brockner, W. *Heteroatom Chem.* **1990**, *1*, 357−362. (b) Toffoli, P.; Khodadad, P.; Rodier, N. *Acta Crystallogr., Sect. B: Struct. Sci.* **1977**, *B33*, 1492−1494. (c) Toffoli, P.; Khodadad, P.; Rodier, N. *Acta Crystallogr., Sect. B: Struct. Sci.* **1982**, *B38*, 2374−2378. (d) Jandali, M. Z.; Eulenberger, G.; Hahn, H. *Z. Anorg. Allg. Chem.* **1978**, *445*, 184−192. (e) Durand, E.; Evain, M.; Brec, R. *J. Solid State Chem.* **1993**, *102*, 146−155. (f) McCarthy, T.; Kanatzidis, M. G. *J. Alloys Compd.* **1996**, *236*, 70−85. (g) Hess, R. F.; Gordon, P. L.; Tait, D.; Abney, K. D.; Dorhout, P. K. *J. Am. Chem. Soc.* **2002**, *124*, 1327−1333.

(16) Hess, R. F.; Abney, K. D.; Burris, J. L.; Hochheimer, H. D.; Dorhout, P. K. *Inorg. Chem.* **2001**, *40*, 2851−2859.

(17) Evain, M.; Brec, R.; Ouvrard, G.; Rouxel, J. *J. Solid State Chem.* **1985**, *56*, 12−20.

(18) Blachnik, R.; Matthiesen, J. Müller, A.; Nowottnick, H.; Reuter, H. *Z. Kristallogr. - New Cryst. Struct.* **1998**, *213*, 233−234.

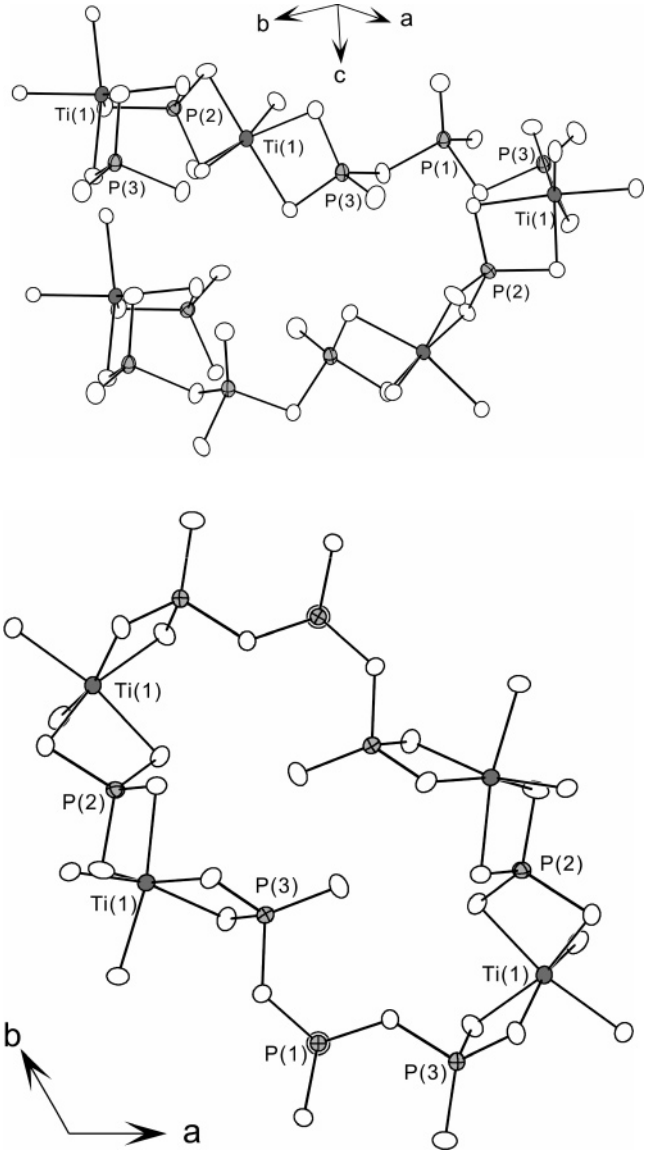

Figure 3. The second helical chain in $Rb_3Ti_3(P_4S_{13})(PS_4)_3$ (**1**) (top) with atomic labeling generating the helical tunnel **II** (bottom). The ellipsoids are drawn at the 70% probability level.

Scheme 1

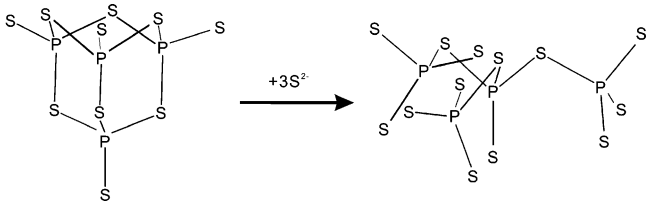

The structure of $Cs_2[Ti_2(P_2S_8)(PS_4)_2]$ (**2**) is another example for a three-dimensional network constructed by the interconnection of $[TiS_6]$ octahedra and two types of thiophosphate ligands, namely the $[PS_4]^{3-}$ anion and the rarely observed $[P_2S_8]^{4-}$ group, which form polar tunnels parallel to the crystallographic *b*-axis. The Cs^+ cations reside in these tunnels as depicted in Figure 4.

In the structure 2 unique Cs atoms, 2 Ti atoms, 4 P atoms, and 16 S atoms are on general positions. The two crystallographically independent Cs^+ cations show their expected high coordination numbers with nine Cs(1)−S and seven

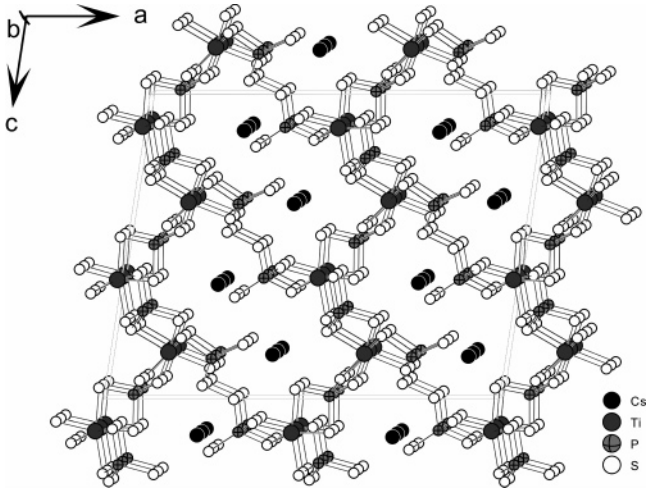

Figure 4. Crystal structure of $Cs_2[Ti_2(P_2S_8)(PS_4)_2]$ (**2**) with the view down [010].

Cs(2)−S bonds in the range between 3.5 and 3.9 Å (Cs(1)−S: 3.5886(19)−3.8142(18) Å, average: 3.683 Å; Cs(2)−S: 3.6791(15)−3.8908(18) Å, average: 3.772 Å). Two of the four P atoms (P(1) and P(2)) belong to a $[P_2S_8]^{4-}$ bithiophosphate anion, in which two $[PS_4]$ tetrahedra are joined by a S−S bond. Hence this anion may be also described with the formula $[P_2S_6(S_2)]^{4-}$. The remaining two P atoms form $[PS_4]$ tetrahedra. In the structure the two independent Ti atoms each share edges with three PS_4 tetrahedra (Ti(1): P(2,3,4); Ti(2): P(1,3,4)) to form TiS_6 octahedra. Adjacent Ti atoms are bridged either by the $[P(4)S_4]$ tetrahedron or by the $[P_2S_8]$ group yielding a one-dimensional undulated chain being directed along [100]. Within the chain the sequence of the building groups is $-Ti(1)-P_2S_8-Ti(2)-P(4)S_4-Ti(1)-$ (see Figure 5, top). Neighbored chains are joined by the $[P(3)S_4]$ tetrahedron to form the three-dimensional network with polar tunnels running along [010] (Figure 5, bottom). The tunnels with an elliptical shape have a diameter of 4·11 Å (measured from coordinate to coordinate).

The Ti−S distances (range: 2.4099(19)−2.4657(19) Å; average: 2.434(2) Å) are almost identical to that in **1** or $K_3Ti_2P_5S_{18}$[4]. Like in compound **1** the S−Ti−S angles clearly demonstrate a significant distortion (Table 3) which is caused by the connection mode between $[PS_4]$ tetrahedra and the TiS_6 octahedra.

The bithiophosphate $[P_2S_8]^{4-}$ unit consists of two PS_4 tetrahedra linked by a S_2^{2-} anion, and this anion has been previously observed in V_2PS_{10}[19] and Nb_2PS_{10}.[20] As in compound **1** and other quaternary thiophosphates,[4] the P−S distances in the $[P_2S_8]^{4-}$ anion can be divided into three sets: (i) P−S(3, 6) to terminal S atoms are the shortest bonds with 1.957(2) and 1.954(2) Å; (ii) P−S(1, 2, 7, 8) bonds to S atoms which are also bound to the Ti atoms have intermediate values (Table 3); and (iii) P−S(4, 5) bonds to S atoms of the disulfide anion are the longest with 2.132(2)

(19) Brec, R.; Ouvrard, G.; Evain, M.; Grenouilleau, P.; Rouxel, J. *J. Solid State Chem.* **1983**, *47*, 174−184.
(20) Brec, R.; Grenouilleau, P.; Evain, M.; Rouxel, J. *Rev. Chim. Min.* **1983**, *20*, 295−304.

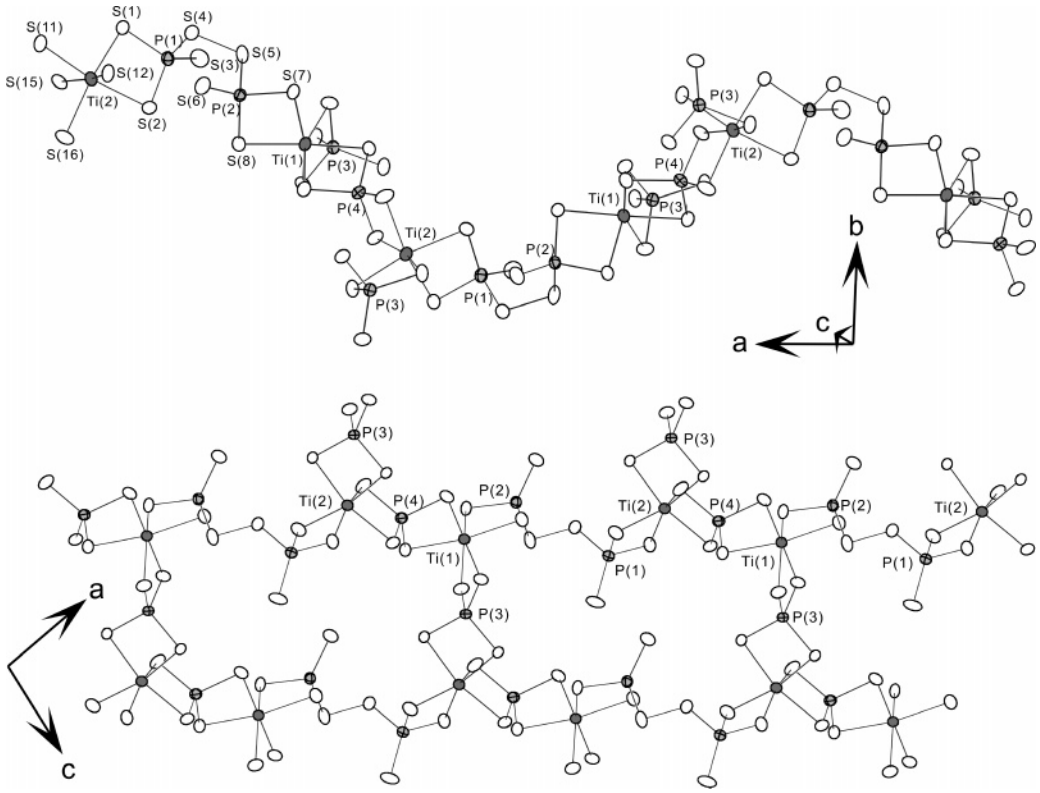

Figure 5. A section of the tunnel in the structure of $Cs_2Ti_2(P_2S_8)(PS_4)_2$ (**2**) with atomic labeling. The ellipsoids are depicted at the 70% probability level.

and 2.147(2) Å. The S−S distance of 2.033(2) Å is typical for S_2^{2-} groups. The average terminal P−S distance of 1.956(2) Å in **2** is significantly shorter than the average P−S bond (2.136(2) Å) to the S atoms of the S_2^{2-} unit. A comparable trend has been observed for other thiophosphates with terminal S atoms and S_n^{2-} groups as part of the thiophosphate anion. The compounds M_2PS_{10} (M = V,[19] Nb[20]) contain the $[P_2S_8]^{4-}$ anion with the S_2^{2-} unit. The average bond lengths to terminal and bridging S atoms are 2.014(5) and 2.127(3) Å for M = V and 2.023(3) and 2.107(2) Å for M = Nb. $Nb_4P_2S_{21}$[21] and $K_4Ti_2P_6S_{25}$[4] contain the $[P_2S_9]^{4-}$ group with a S_3^{2-} anion joining two PS_4 tetrahedra. The values reported for the average $P-S_{term}$ and $P-S_{br}$ bonds are 2.026(3) and 2.117(2) Å for $Nb_4P_2S_{21}$ and 1.964 and 2.147 Å for $K_4Ti_2P_6S_{25}$.[4] In $Cs_4P_2S_{10}$[22] the $[P_2S_{10}]^{4-}$ anion contains a S_4^{2-} unit bridging the two PS_4 tetrahedra. The average $P-S_{term}$ bond length amounts to 2.005(6) Å and that for the bridging P−S distance to 2.192(6) Å.

The S−P−S angles in **2** cover a relatively large range from 95.55(9)° to 119.98(11)° (Table 3) giving evidence for a significant distortion.

Comparing the structures of **1** and **2**, the tunnel in the $[Ti_2(P_2S_8)(PS_4)_2]^{2-}$ anion shows some similarity to tunnel **II** in $Rb_3Ti_3(P_4S_{13})(PS_4)_3$. But the arrangement and connection modes of the building units in the chain forming the tunnel in **2** are different as discussed above. The structures accommodate the cations within the tunnels. In **1**, the site in tunnel **I** is occupied by Rb(2) ions to a low extent (see above). One reason for this low occupancy may be that the $Rb(2)S_6$ octahedra share triangular faces which would lead to strong repulsive interactions if more Rb(2) is located on this site. The introduction of the larger Cs^+ ions would increase these repulsive forces destabilizing the structure. Furthermore, the size of the octahedral void in tunnel **I** is just large enough to host the smaller Rb^+ ion (see average Rb−S and Cs−S bond lengths). With analysis of the chemical composition of the two compounds another difference becomes obvious. The ratio A:Ti:P:S (A = Rb, Cs) is different in the two compounds which can be rationalized by doubling the formula of compound **1** yielding $Rb_6Ti_6P_{14}S_{50}$ and tripling the formula of compound **2** ($Cs_6Ti_6P_{12}S_{48}$). Charge compensation in compound **2** is achieved by the formation of three S_2^{2-} ions. In the syntheses the ratios of $A_2S_3/Ti/P_2S_5/S$ were identical for both compounds. The occurrence of $[P_4S_{13}]^{6-}$ in **1** and of $[P_2S_8]^{4-}$ in **2** may be due to a combination of the cation size effect and the slightly more oxidizing nature of the $Cs_2S_3/P_2S_5/S$ flux. The slightly more oxidizing $Cs_2P_4S_{18}$ flux favors the formation of S_2^{2-} which forms the $[P_2S_8]^{4-}$ building block, whereas in the less oxidizing $Rb_2P_4S_{18}$ flux the $[P_4S_{13}]^{6-}$ anion is stabilized. Changing the flux conditions ($Rb_2S_3/P_2S_5/S$ = 1:1:5) yielded $RbTiPS_5$, which contains one S^{2-} per formula unit.[3a]

3.2. Optical Properties. The UV/vis spectra of compounds **1** and **2** (Figure 6) show a steep absorption edge, and the band gaps E_g are estimated to 1.70 eV for **1** and 1.73 eV for **2**. These data are in agreement with the black color of the samples.

(21) Brec, R.; Evain, M.; Grenouilleau, P.; Rouxel, J. *Rev. Chim. Min.* **1983**, *20*, 283−294.
(22) Aitken, J. A.; Canlas, C.; Weliky, D. P.; Kanatzidis, M. G. *Inorg. Chem.* **2001**, *40*, 6496−6498.

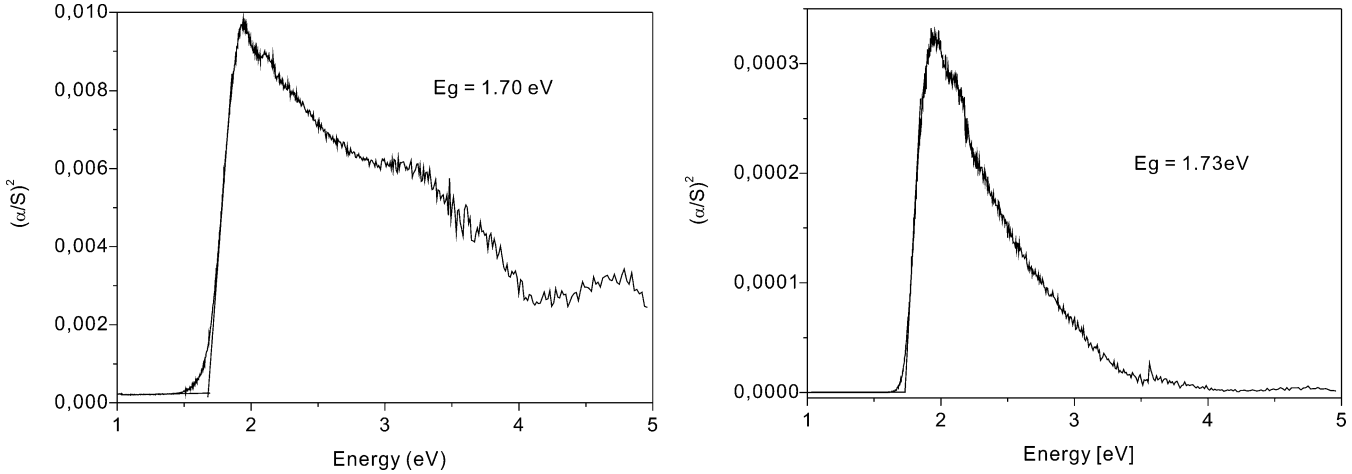

Figure 6. Transformed reflectance spectra of $Rb_3Ti_3(P_4S_{13})(PS_4)_3$ (**1**) (left) and $Cs_2Ti_2(P_2S_8)(PS_4)_2$ (2) (right).

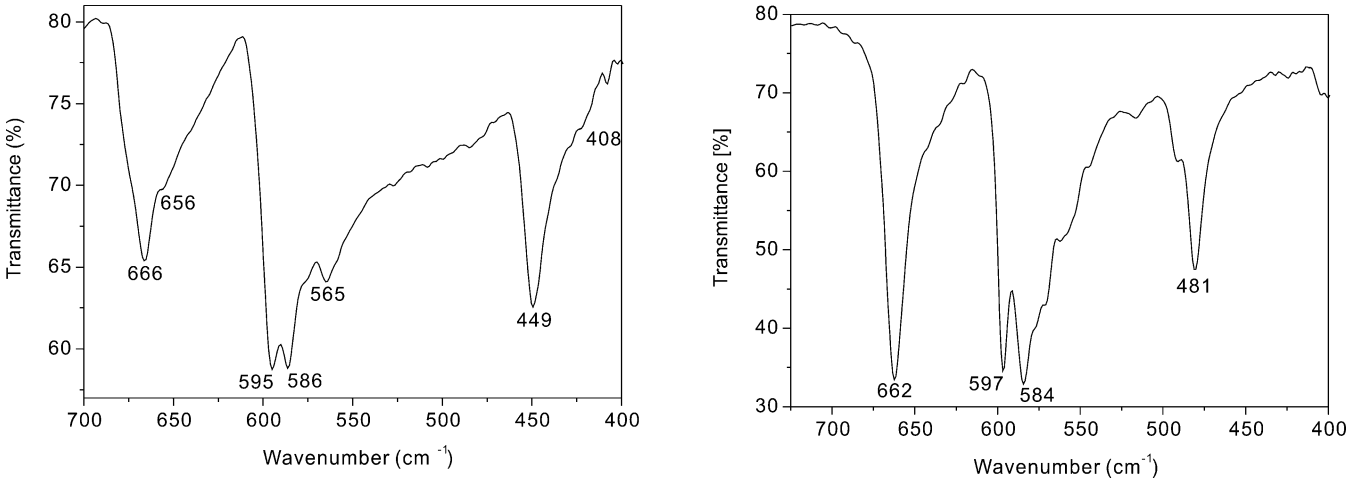

Figure 7. MIR spectra of $Rb_3Ti_3(P_4S_{13})(PS_4)_3$ (**1**) (left) and $Cs_2Ti_2(P_2S_8)(PS_4)_2$ (**2**) (right).

The MIR spectra of compounds **1** and **2** are shown in Figure 7. For **1**, absorptions at 666, 656, 595, 586, 565, 449, and 408 cm^{-1} are seen. The spectroscopic relevant units are the $[P_4S_{13}]^{6-}$ and the $[PS_4]^{3-}$ anion. Based on the pseudotetrahedral symmetry of these units, the signal at 449 cm^{-1} is assigned to a P−S−P stretching vibration. The remaining absorptions are due to P−S stretching modes. Similar patterns were found in the IR spectra of $K_3M_2P_5S_{18}$ (M = Sn, Ti)[4] and $Cs_3Zr_2P_5S_{18}$.[5]

The MIR and FIR (not shown) spectra of $Cs_2Ti_2(P_2S_8)(PS_4)_2$ (**2**) exhibit absorptions at 662, 597, 584, 481 cm^{-1} and 480, 399, 321, 306 256, 216 cm^{-1}, respectively. The absorption at 481 (FIR: 480) cm^{-1} with a shoulder at higher energy is assigned to an asymmetric S−S stretching vibration, which was also found in the IR spectrum of $(NH_4)_2(Mo_3S(S_2)_6$.[22] Similar to compound **1**, the remaining signals above 300 cm^{-1} are due to P−S stretching vibrations, absorption bands below 300 cm^{-1} to PS_4 bending and Ti−S stretching vibrations.

The Raman spectra of $Rb_3Ti_3(P_4S_{13})(PS_4)_3$ (**1**) and $Cs_2Ti_2(P_2S_8)(PS_4)_2$ (**2**) are shown in Figure 8. It is difficult to unambiguously assign all the Raman peaks since expected vibrations for PS_4 and/or S_2^{2-} fragments overlap in certain regions. If the intensities of peaks are not considered, both Raman spectra show a high similarity except the peaks in the region between 450 and 550 cm^{-1}. Combined with their MIR spectra, the resonances at 676, 656, 600, 583, 566, 428, 396, 363, and 327 cm^{-1} for compound **1** and at 669, 595, 571, 554, 544, 423, 404, 352, and 325 cm^{-1} for compound **2** can be tentatively assigned to P−S stretching vibrations. Compared to other PS_4 containing compounds,[23] the first five peaks in the spectra of **1** and **2** shifted to slightly higher energies. This shift may be caused by the shorter terminal P−S bonds in the $[P_4S_{13}]^{6-}$ and $[P_2S_8]^{4-}$ anions. The remaining resonances occur at positions being typical for "normal" P−S bonds. Absorptions below 300 cm^{-1} for both compounds are due to Ti−S stretching vibrations and P−S deformation modes. The intense peaks at 472 and 450 cm^{-1} in the spectrum of **1** are assigned to the P−S−P stretching vibrations by analogy to $Ag_4P_2S_7$[15b] and $KAuP_2S_7$,[25] whereas the relative weak peaks at 516 and 484 cm^{-1} may be due to S−S stretching modes.[23]

(23) Müller, A.; Haegermann, W.; Enemark, J. H. *Coord. Chem. Rev.* **1982**, *46*, 245−280.
(24) Derstroff, V.; Ensling, J.; Ksenofonov, V.; Gütlich, P.; Tremel, W. *Z. Anorg. Allg. Chem.* **2002**, *628*, 1340−1354.
(25) Chondroudis, K.; Hanko, J. A.; Kanatzidis, M. G. *Inorg. Chem.* **1997**, *36*, 2623−2632.

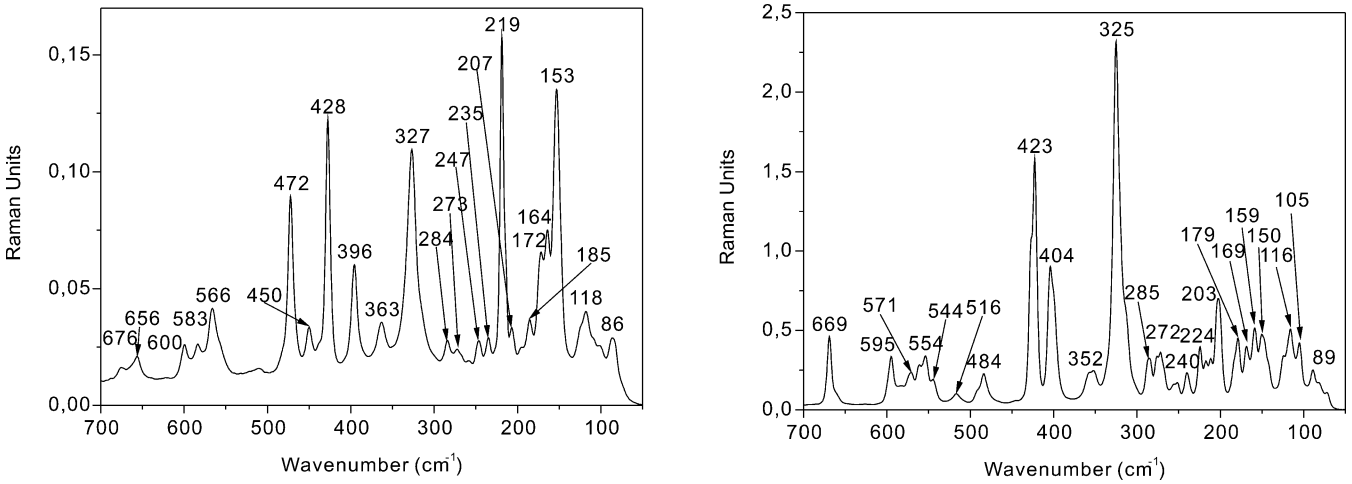

Figure 8. FT-Raman spectra of $Rb_3Ti_3(P_4S_{13})(PS_4)_3$ (**1**) (left) and $Cs_2Ti_2(P_2S_8)(PS_4)_2$ (**2**) (right).

4. Conclusions

The main structural features of two new quaternary Ti thiophosphates are complex one-dimensional polar tunnels. In $Rb_3Ti_3(P_4S_{13})(PS_4)_3$ the previously unknown $[P_4S_{13}]^{6-}$ anion is a fundamental building unit. This anion represents a new member of the $[P_nS_{3n+1}]^{(n+2)-}$ series including the pyrothiophosphates $[P_2S_7]^{4-}$ and $[P_3S_{10}]^{5-}$. Two different types of helical tunnels are constructed by two different helical chains. The structure of $Cs_2Ti_2(P_2S_8)(PS_4)_2$ contains the rarely observed $[P_2S_8]^{4-}$ group besides TiS_6 octahedra and $[PS_4]^{3-}$ anions. Neighbored undulated chains are joined by a $[PS_4]^{3-}$ tetrahedron to form the three-dimensional network with polar tunnels. Both compounds represent further examples for the large potential of syntheses in alkali polythiophosphate fluxes. Under the reaction conditions new structural building groups like the hitherto unknown $[P_4S_{13}]^{6-}$ anion are generated and stabilized in the crystal products. Interestingly, both compounds were obtained in alkali polythiophosphate fluxes under identical synthesis conditions. One can only speculate why $[P_4S_{13}]^{6-}$ is formed in the Rb containing flux, whereas the $[P_2S_8]^{4-}$ group is observed in the Cs compound. The different sizes of the cations as well as the different oxidizing power of the fluxes may be the main synthetic parameters determining the formation of structural building blocks. But more thiophosphate compounds must be prepared under different synthesis conditions to gain more insight into the relation between preparation conditions and the structural motifs in the products.

Acknowledgment. The authors thank Ms. I. Jess and Dr. C. Näther for single-crystal data collections and Ms. U. Cornelissen for measurements on the IR, Raman, and diffuse reflectance instruments. Funding for this work was provided by the State of Schleswig-Holstein, the Fonds der Chemischen Industrie (FCI), and the Deutsche Forschungsgemeinschaft (DFG).

Supporting Information Available: X-ray crystallographic file (in CIF format) for compounds **1** and **2**. This material is available free of charge via the Internet at http://pubs.acs.org.

IC700478R